ISSN 1726-5479

SENSORS & TRANSDUCERS

11/10 vol. 122

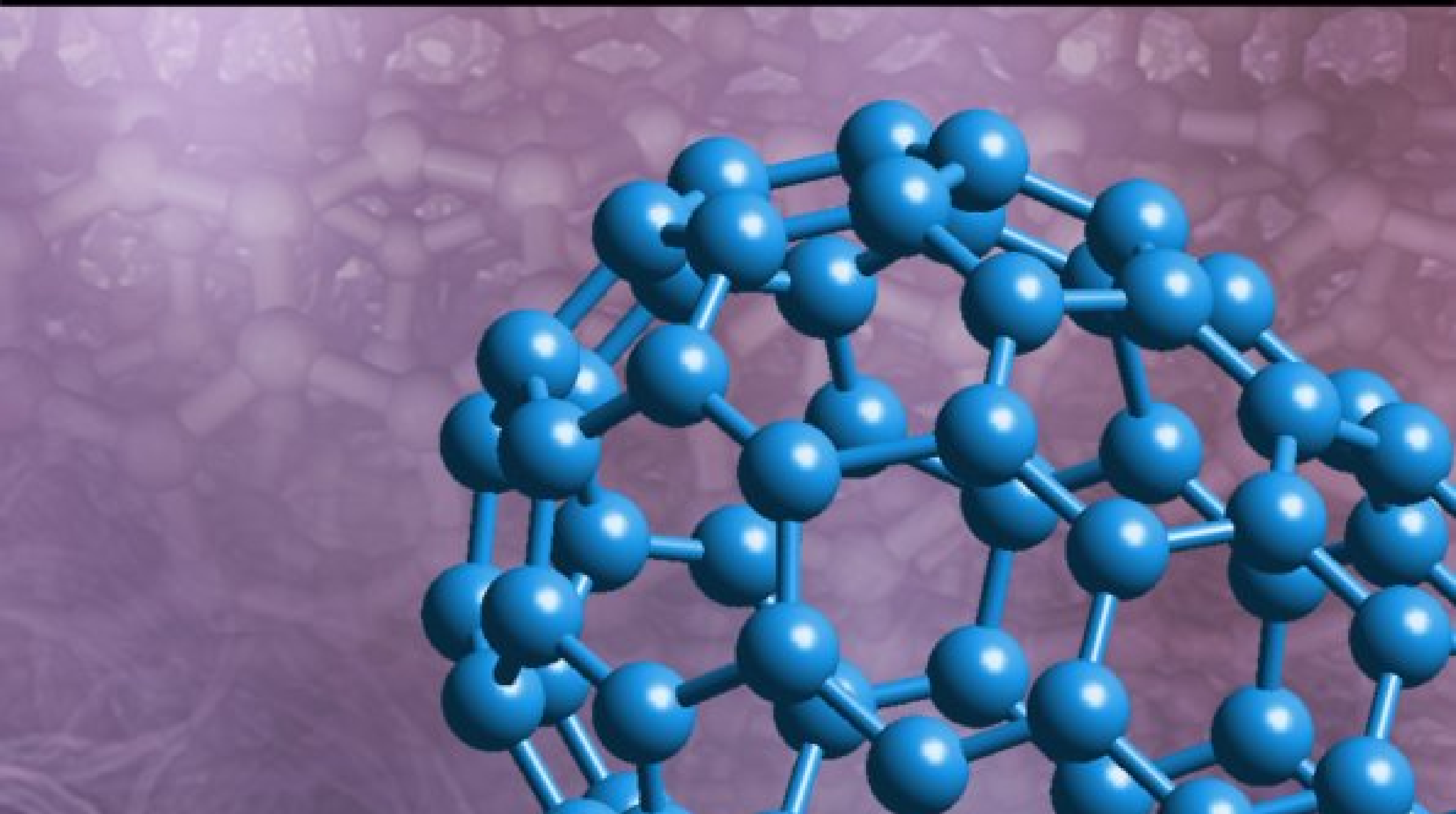

Nanosensors and Nanodevices

International Frequency Sensor Association Publishing

IFSA

Sensors & Transducers

Volume 122, Issue 11, November 2010 www.sensorsportal.com ISSN 1726-5479

Sensors & Transducers Journal

Contents

Volume 122
Issue 11
November 2010

www.sensorsportal.com

ISSN 1726-5479

Research Articles

Authors are encouraged to submit article in MS Word (doc) and Acrobat (pdf) formats by e-mail: editor@sensorsportal.com
Please visit journal's webpage with preparation instructions: http://www.sensorsportal.com/HTML/DIGEST/Submition.htm

International Frequency Sensor Association (IFSA).

Sensors & Transducers Journal, Vol. 122, Issue 11, November 2010, pp. 158-172

www.sensorsportal.com

Sensors & Transducers

ISSN 1726-5479

http://www.sensorsportal.com

Fabrication and Analysis of Tapered Tip Silicon Microneedles for MEMS based Drug Delivery System

[*]Muhammad Waseem Ashraf, Shahzadi Tayyaba, Nitin Afzulpurkar, Asim Nisar
School of Engineering and Technology, Asian Institute of Technology (AIT), Bangkok, Thailand
[*]E-mail: Muhammad.Waseem.Ashraf@ait.ac.th

Received: 26 June 2010 /Accepted: 18 November 2010 /Published: 30 November 2010

Abstract: In this paper, a novel design of transdermal drug delivery (TDD) system is presented. The proposed system consists of controlled electronic circuit and microelectromechanical system (MEMS) based devices like microneedles, micropump, flow sensor, and blood pressure sensor. The aim of this project is to develop a system that can eliminate the limitations associated with oral therapy. In this phase tapered tip silicon microneedles have been fabricated using inductively coupled plasma (ICP) etching technology. Using ANSYS, simulation of microneedles has been conducted before the fabrication process to test the design suitability for TDD. More over multifield analysis of reservoir integrated with microneedle array using piezoelectric actuator has also been performed. The effects of frequency and voltage on actuator and fluid flow rate through 6×6 microneedle array have been investigated. This work provides envisage data to design suitable devices for TDD. *Copyright © 2010 IFSA.*

Keywords: Tapered tip silicon microneedles, Coupledmultifield, Finite element method, Transdermal drug delivery system.

1. Introduction

Transdermal drug delivery (TDD) has been considered as a patient-friendly method to deliver the pharmaceutical compound by eradicating pain, gastrointestinal absorption, liver metabolism and degradation that are associated with conventional drug delivery approaches like hypodermic injections and oral administration of drugs. The use of microelectromechanical systems (MEMS) technology has been increasing rapidly in biomedical devices. Due to MEMS technology, the fabrication of miniature size and soaring performance medical devices has become practicable to congregate the critical medical requirements like controlled delivery with negligible side effects, improved bioavailability and therapeutic effectiveness. The first study for the improvement of TDD was conducted by inserting the microneedle in cadaver skin [1]. The microneedles have different design according to their lengths, structure, shape, array density and materials [2]. The detail of microneedle categories is shown in Table 1.

Table 1. Categories of microneedles.

Material	Overall shape	Tip shape	Structure	Application
Silicon	Cylindrical	Volcano	Hollow	Drug delivery
Silicon dioxide	Pyramid	Snake fang	Solid	Blood extraction
Silicon nitride	Candle	Micro- hypodermis	In-plane	Fluid sampling
Glass	Spike	Tapered	Out-of-plane	Cancer therapy
Semiconductor	Spear			Micro-dialysis
Metals	Square			Ink-jet-printing
Alloys				Sensing
Polymers				

The earliest out-of-plane microneedle array consisted of 100 microneedles with a length of 1.5 mm was reported in 1991 [3]. The tetrahedron sharp tip in-plane microneedles reported for TDD [4]. Different techniques have been described in literature to fabricate microneedles like photolithography [5], deep x-ray lithography [6], deep reactive ion etching (DRIE) [7], micro-molding [8], bi-mask technique [9], surface micromachining [10], LIGA [11], hot embossing [12], UV excimer laser [13], laser micromachining [14], coherent porous silicon etching (CPS) [15], Injection molding [16] and micropipette pulling technique [17]. In these processes, silicon and polymer can be used as substrate materials for microfabrication. However, application of silicon as the substrate material is still dominant because of some excellent mechanical properties, electrical properties and possibility to directly integrate circuit on the transducer's substrate.

In past, various studies have been done on the design, analysis and fabrication of MEMS based microneedles, micropumps and miniature mixer for TDD applications. However, only few have been converted as commercial products. The main reasons are the complications of bio-MEMS devices, difficulties in integration with other devices and finally packaging is the great challenge. MEMS based integrated TDD system consists of microneedles, micropump, blood pressure sensor, flow sensors, and electronic circuits. A simplified block diagram of proposed integrated TDD system is shown in Fig. 1.

Electronic module provides the required circuitry. Blood pressure sensor monitors the patient's blood pressure. Based on the results and requirements, TDD automatically injects the desired dose of drug into patient's body. To insure the safety of patient, the flow sensor accomplishes the real time sensing of release volume of drug. The flow of drug is scrutinized by the flow sensor to avoid the large vacillation of flow rate. Drug delivery device consists of piezoelectric actuator and a reservoir integrated with microneedle array. Actuator provides actuation mechanism to vibrate the membrane. Reservoir provides drug storage and microneedles provide the interface between TDD system and patient's body to liberate the drug.

In this study, the authors present the fabrication of tapered tip hollow out-of-plane silicon microneedles and multifield analysis of reservoir integrated with 6×6 microneedle array for TDD system. In integrated device the reservoir and piezoelectric actuator behave like micropump. The in-depth numerical analysis of piezoelectric valveless micropump [18] and fabrication of piezoelectric micropump were been done [19] in the first stage of project. The analysis shows that the fabricated microneedles can be integrated with our fabricated micropump. In coupledfield analysis, the effect of frequency and voltage on the deflection of piezoelectric actuator and fluid flow rate through microneedles is studied.

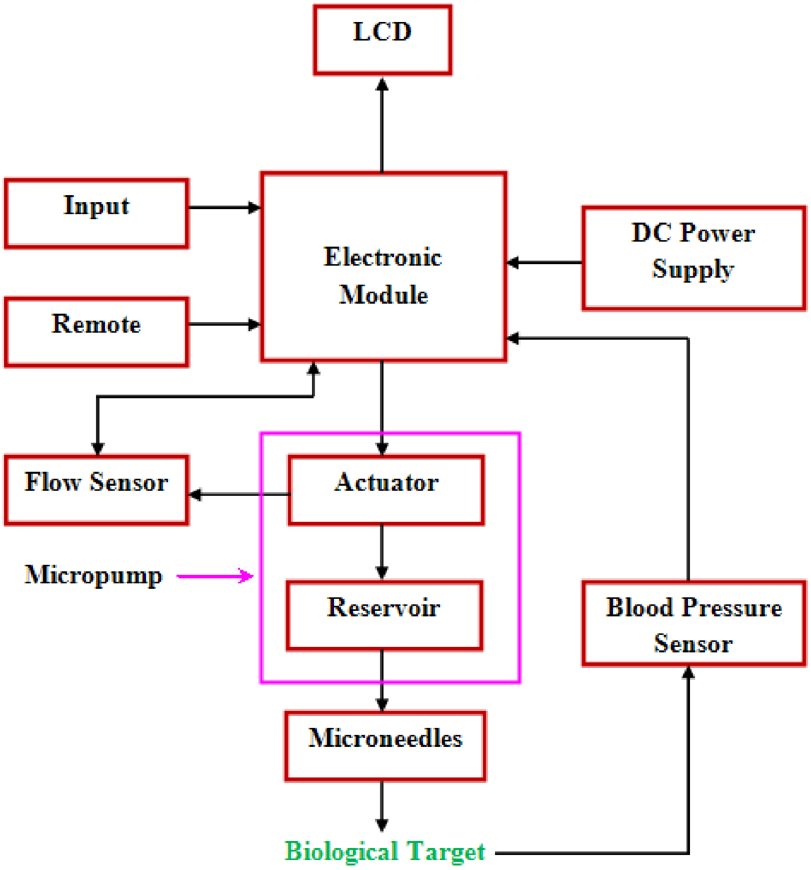

Fig. 1. Block diagram of drug delivery system.

2. Fabrication

The microneedle design is cylindrical with tapered tip section, which provides enough strength and ease of skin insertion. Combination of isotropic and anisotropic etching has been used to fabricate tapered tip hollow out-of-plane silicon microneedles in inductively coupled plasma (ICP) etcher. Required shape of microneedles has been accomplished by controlling the etch time at different processing steps. The DRIE process parameters are shown in Table 2.

Table 2. DRIE process parameters.

DRIE (Bosch process parameters)	**Etching from front side**	**Etching from back side**
Temperature (^{o}C)	15	20
Etching time (min)	15	25
Stop time (min)	3	3
Power RF (W)	1400	1600
Etching/Passivation		
Flux SF_6/C_4F_8 (sccm)	250/150	250/100
Pressure SF_6 (Pa)	3.5	4

Various steps were involved during microneedles fabrication process. In first step, 6 inch silicon wafer was cleaned (Fig. 2a). Then silicon wafer was blown dry with air gun. The second step was to cap photoresist mask (Fig. 2b). This step involved various substeps such as spin coating photoresist AZ4620 @3000 rpm, soft bake (100-150 sec @ 100 ^{0}C), expose wafer, develop in developer solution

AZ 400K and hard bake. Then isotropic dry etching was done in ICP etcher using SF_6/O_2 gases for tip and outside shape of microneedle in standard photolithography process (Fig. 2 c, d, e). The first etch depth was 15 μm. Then photoresist is stripped off and wafer is cleaned. The next step is to thermally grown silicon oxide layer on the wafer in oxidation furnace by wet oxidation at 1000 ^{0}C. Then wafer is protected by capping with another wafer for mask oxide etching. Then photoresist was striped. To fabricate the inner hole the ICP etching was performed. The photoresist was first coated with 5 μm thickness. The etching depth for first ICP etch is 150 μm. This is followed by second ICP etch up to 200 μm (Fig. 2f). The final step involved release, oxide etch and dicing. The fabricated microneedles are shown in results and discussion section of the paper. The fabrication process flow of microneedles is shown in Fig. 2.

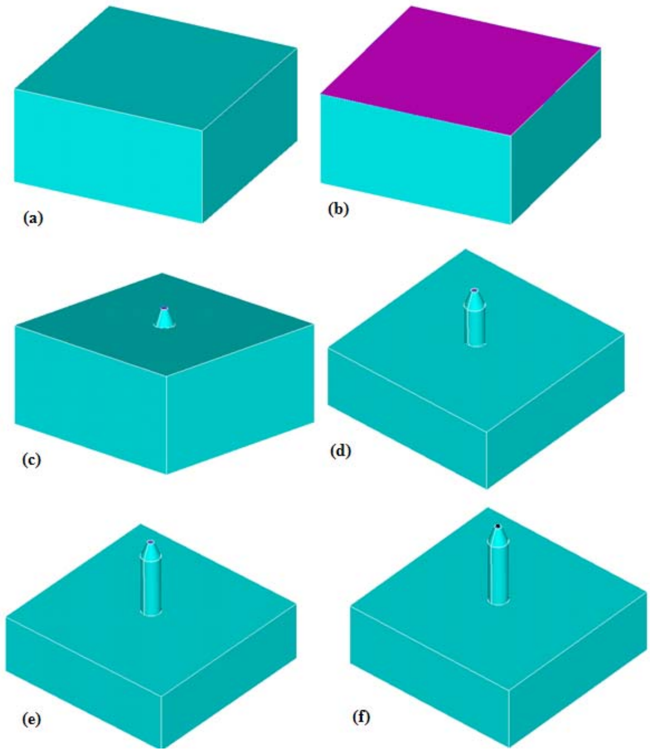

Fig. 2. Fabrication process flow.

3. Theoretical Analysis

Microneedle design is cylindrical with tapered tip as shown in Fig. 3. P_1 and P_2 are the inlet and outlet pressure of the microneedle. D represents the tip diameter of microneedle. D_1 and D_2 represent internal and outer diameter of microneedle. L is the length of the microneedle and Q is the flow rate in the lumen section.

3.1. Mechanics of Microneedle

Microneedle can be broken during insertion because various forces are acting on the needles like bending, buckling, axial, and resistive forces. An axial force is experienced on the tip of microneedle. This force may cause buckling of the microneedle. F_{axial} is the force which the microneedles can withstand without fracture as shown:

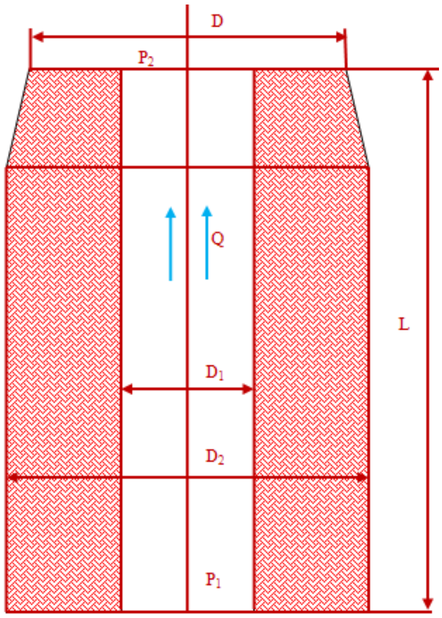

Fig. 3. Cross section of microneedle.

$$F_{axial} = \sigma_y A \ , \tag{1}$$

where σ_y is the yield strength, A is the cross-sectional area of needle tip.

Human skin offers the resistive forces against the microneedle penetration. The pressure on the microneedle should be greater than the resistive forces. $F_{resistance}$ before the skin punctured is expressed by the following equation:

$$F_{resistance} = P_{pierce} A \, , \tag{2}$$

where P_{pierce} is the required pressure to puncture the skin.

Fractional forces are experienced by the microneedles after the penetration into human skin. These forces arise because tissues and microneedle contact. $F_{Bending}$ is the force which microneedle can withstand without breaking shown as:

$$F_{Bending} = \frac{\sigma_y I}{cL} \, , \tag{3}$$

where L is the length of microneedle.

3.2. Fluidic Analysis

Fluid flow characteristics are extremely important because array of microneedle is used to inject the drug into human skin. Fluid pressure drop through the microneedle array is based on various reasons like microneedle array geometry, roughness of surface fluid viscosity, and microneedle array density. The dimensions of microneedles are in micron, so the behavior of fluid flow is different from macro level. There is significant resistance to fluid flow through the microneedles. Poiseulle's law is considered to measure the fluid flow through microneedle array as shown below:

$$Q = \frac{\pi D_1^4 (\nabla p)}{64\mu(L)} \tag{4}$$

where Q is the flow rate, D_1 is the diameter of microneedle and μ is the viscosity.

Modified Bernoulli equation is considered to model the microneedles geometry. The pressure loss is calculated by considering the friction losses given by [20]:

$$\frac{P_1}{\rho g} + \frac{V_1}{2g} + Z_1 = \frac{P_2}{\rho g} + \frac{V_2}{2g} + Z_2 + \frac{fl}{d} + \frac{V^2}{2g} + \sum \frac{kV^2}{2g} \tag{5}$$

where P_1 is the inlet pressure, P_2 is the outlet pressure, V_1 is the inlet velocity and V_2 is the outlet velocity.

4. Numerical Simulation

In this study, structural and fluidic analysis has been conducted using ANSYS. Single microneedle was considered for structural analysis. For transient multifield analysis 6×6 microneedle array was considered.

4.1. Structural Analysis

Finite element method (FEM) was used to perform the structural analysis. Single out-of-plane needle was modeled using element SOLID 186. The base of needle is fixed in all direction. Tip of microneedle is allowed free to move during analysis. The young modulus of 169 GPa and Poisson ratio of 0.22 were used for FEM analysis [21, 22]. In the simulation study, bending and axial stress analyses were performed by applying transverse and axial loads respectively. The range of transverse load is assumed according to the fracture strength of the material. For stress analysis the bottom of the microneedle was taken into consideration with applied tip force 8.8 N as shown in Fig. 4.

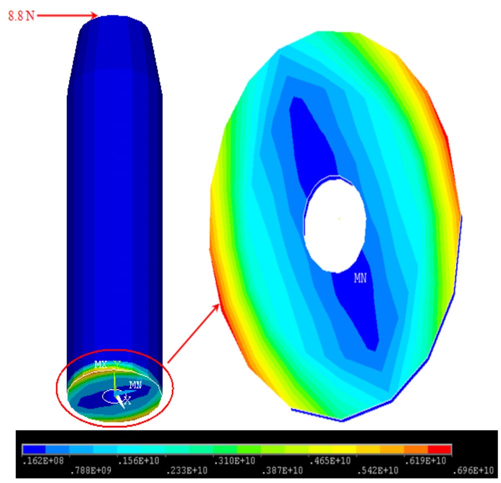

Fig. 4. Bending stress analysis.

Results show maximum stress of 6.96 GPa occurs at inner part of tip that is less than the yield strength of materials. Human skin resistance is 3.18 MPa during needle penetration [23, 24]. So microneedle is strong enough to bear load more than 3.18 MPa. The effect of applied pressure on tip of microneedle is shown in Fig. 5.

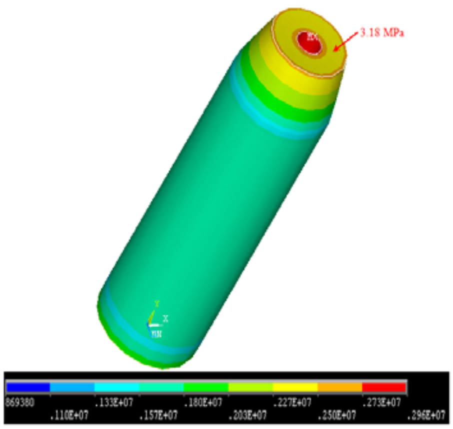

Fig. 5. Axial stress analysis.

Simulation results of axial stress analysis shows that the maximum stress 2.96 MPa occurs inside the lumen section of the microneedle at applied pressure of 3.18 MPa with negligible deflection.

4.2. CFD Analysis at Different Inlet Pressures

Simulation shows the effect of different applied inlet pressures on the flow rate. Single row of microneedle array (6 microneedles) was considered for analysis. The static pressure 20 kPa to 140 kPa was applied at the microneedle inlet. Isothermal fluid domain was chosen for analysis during the simulation. Ethanol was considered for flow analysis in isothermal domain. The simulation results for the applied inlet static pressure are shown in Fig. 6.

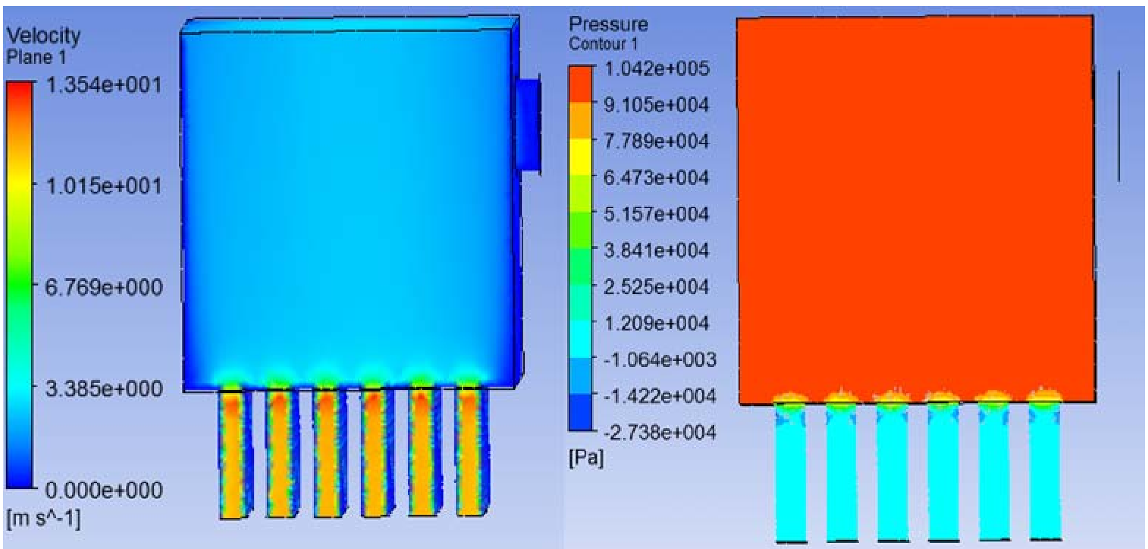

Fig. 6. Velocity and pressure distribution in CFD static analysis.

The result shows that the fluid velocity is negligible in the reservoir due to large area. Velocity of fluid increases in the microneedle lumen section and along the length due to small area [25]. Due to frictional losses between fluid and wall, the fluid velocity is less near wall as compared to the central region of lumen section. Pressure is high and remains constant in the reservoir. It decreases in the lumen because the fluid is flowing towards the outlet (Pressure at outlet = 0 kPa).

4.3. Transient Multifield Analysis

In this analysis, fluid model and structural piezoelectric actuator model were created in ANSYS separately. Then these mechanical inputs were solved in ANSYS mechanical APDL product launcher using MFX-ANSYS/CFX environment. Multiple code coupling method was used in this analysis [26]. The element Brick-20node-226 and SLOID-20node-186 were considered for PZT4 disk and silicon membrane. Circuit-124 element was considered for sinusoidal voltage degree of freedom. The elements Facet 200 and FLOTRAN CFD 142 were considered to create 3D fluid model. Ethanol was assumed as working fluid in isothermal domain. The thickness of the piezoelectric disk and silicon membrane was 200 μm each. The complete model of device is shown in Fig. 7.

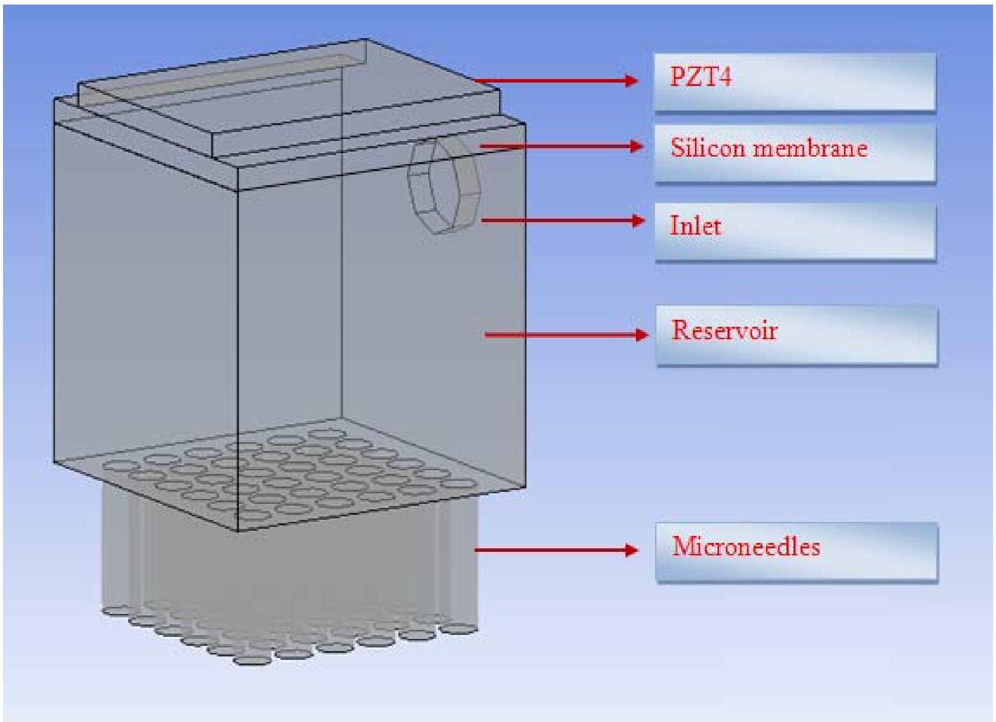

Fig. 7. CFD model of integrated device.

Boundary conditions applied on the device are shown in Fig. 8 [26].

The simulation results of multifield analysis (piezoelectric actuator and fluid model) are shown in Fig. 9. Simulation results show that the actuator has maximum deflection at the center. In fluid model fluid flows in the central region, while near the walls flow is negligible because of frictional forces.

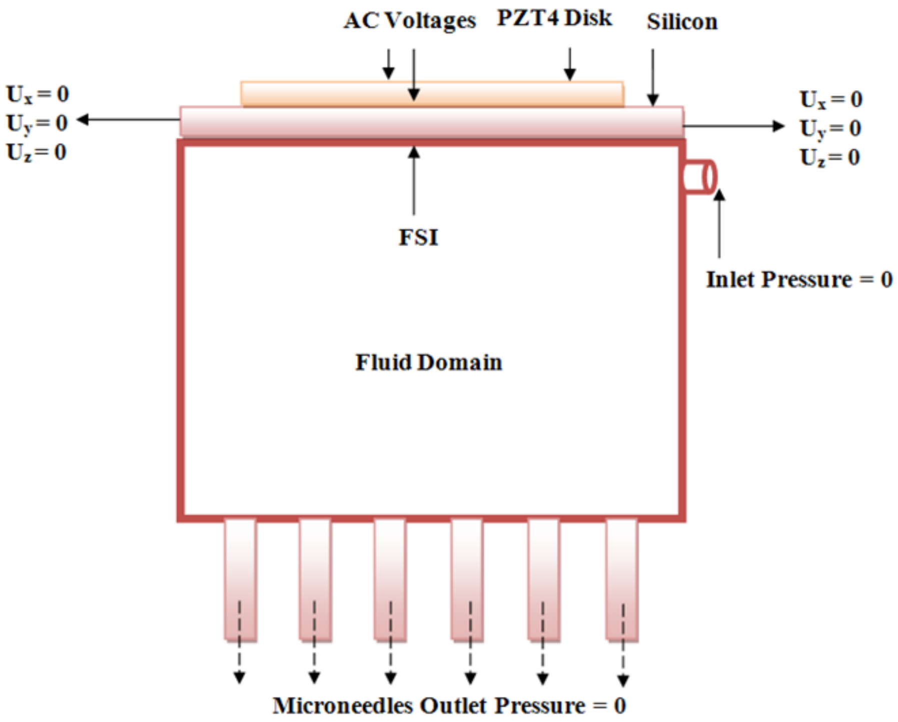

Fig. 8. Boundary condition on integrated device.

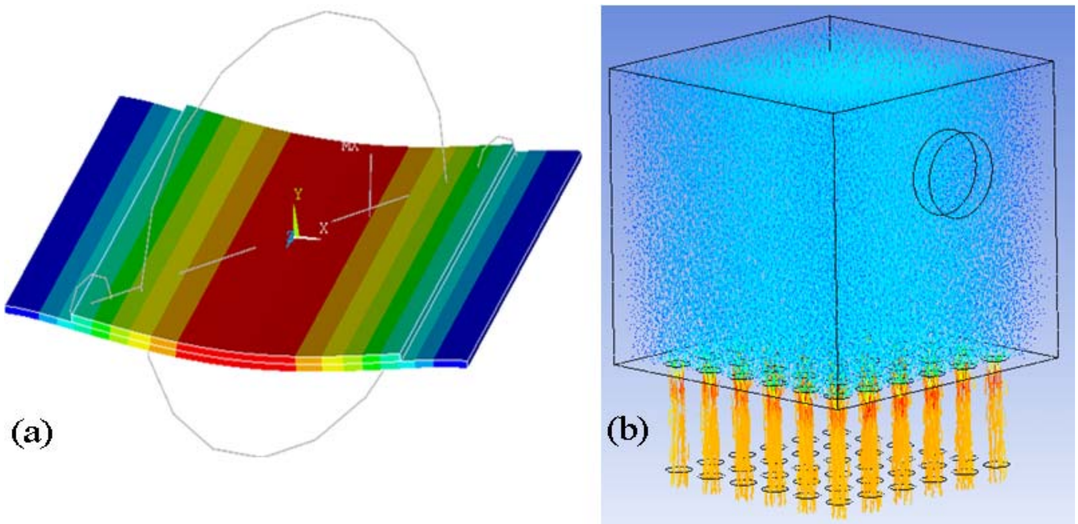

Fig. 9. Multifield simulation results.

5. Results and Discussion

Tapered tip hollow out-of-plane silicon microneedles were fabricated successfully. The length of microneedle is 200 μm to avoid contact of microneedle with sensory organs. The internal diameter of microneedle is 40 μm. The centre-to-centre distance in microneedle array is 750 μm. The scanning electron microscope (SEM) images of fabricated microneedle are shown in Fig. 10.

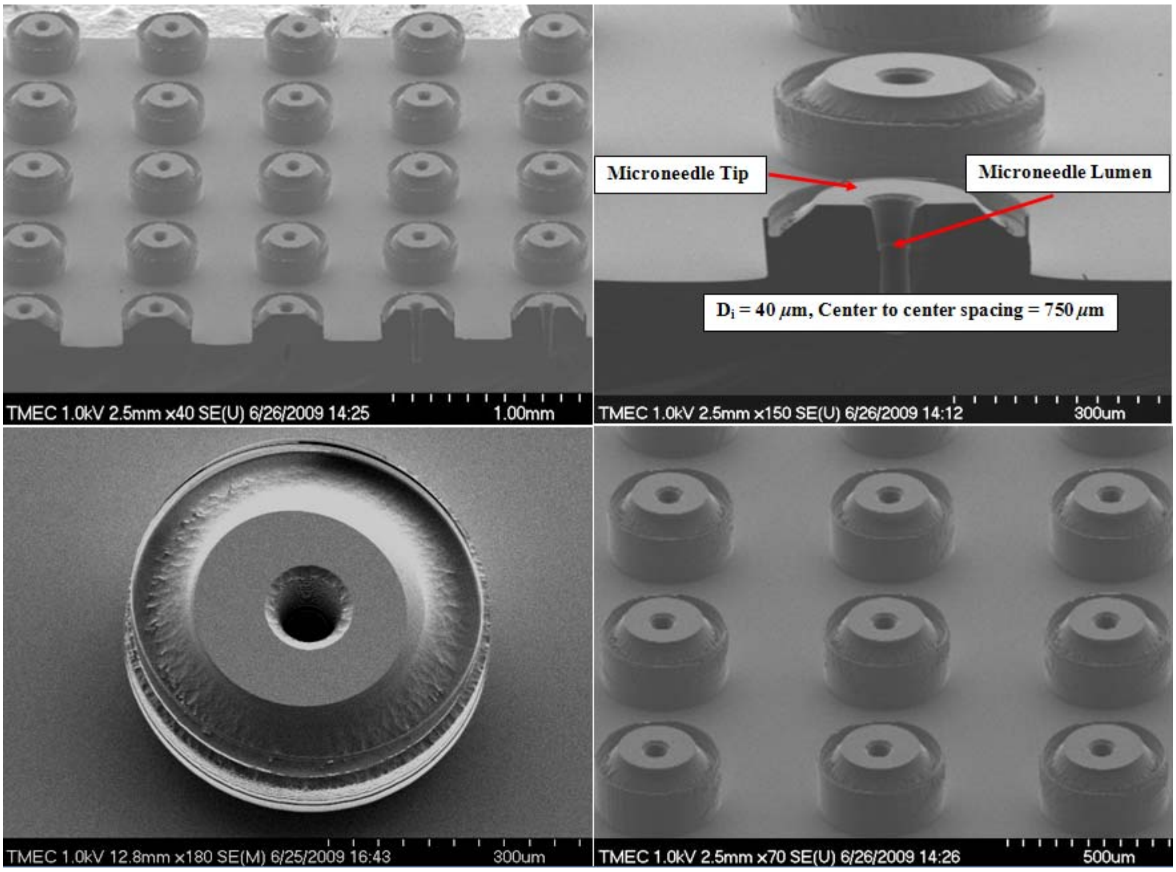

Fig. 10. SEM images of microneedles.

During structural analysis it was found that 6.69 GPa stress occurs at the microneedle bottom with 20 μm deflection at the tip for applied force of 8.8 N. The relation between stress and deflection at applied force is shown in Fig. 11.

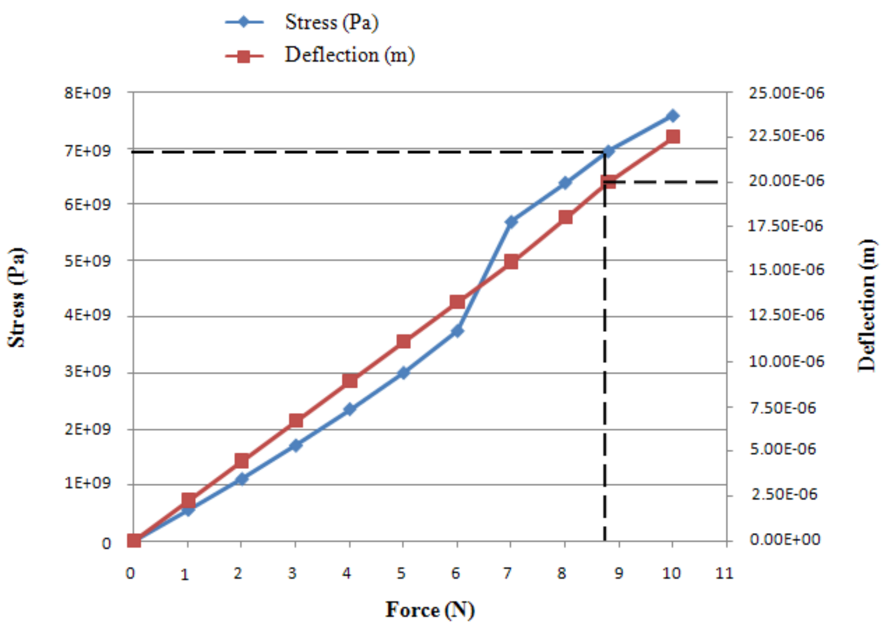

Fig. 11. Stress vs. deflection at applied bending force.

The microneedle fails if the stress value exceeds the yield stress of the material. Results show that maximum stress is less than the yield stress. So, microneedle is strong enough to bear the force up to 8.8 N.

In static CFD analysis, flow rate at various applied pressures is shown in Fig. 12. Fluid flow increases with the increase in inlet pressure. The maximum flow rate 1375 μL/min is observed at 140 kPa.

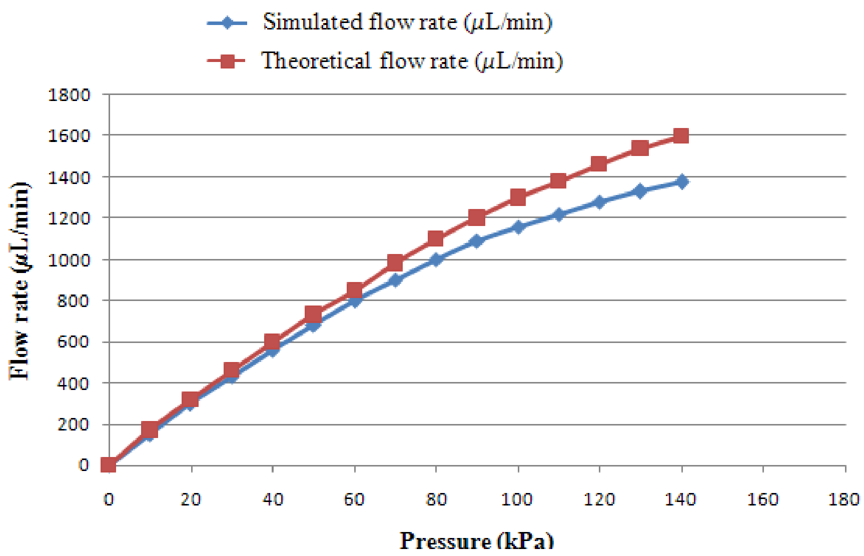

Fig. 12. Fluid flow at applied pressures.

The pressure variation in CFD analysis through the microfluidic device is shown by the Fig. 13. Pressure is high and remains constant through the reservoir because of large area and decreases in the lumen region because of small area and considered zero at the outer end.

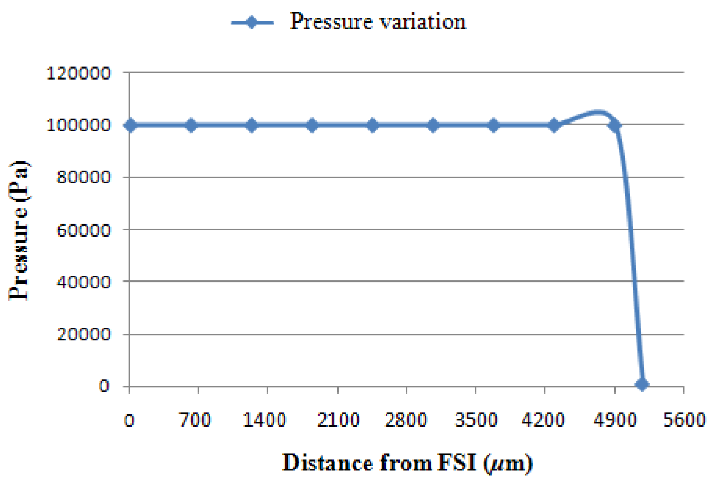

Fig. 13. Pressures variation.

The velocity variation in CFD analysis through the device is shown by the Fig. 14. Initially velocity is little high at first stroke volume and then remains constant through the reservoir because of large area and increases in the lumen region because of small area.

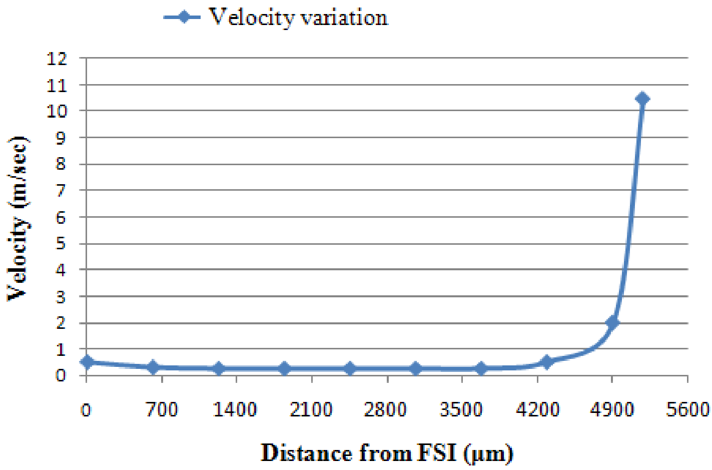

Fig. 14. Velocity variation.

In FEM analysis the bending of actuator at sinusoidal applied 100 V is shown in Fig. 15. The frequency of 250 Hz was considered constant. The deformation is calculated along the length of the actuator. The maximum displacement of 12.24 μm occurs at the centre of the membrane.

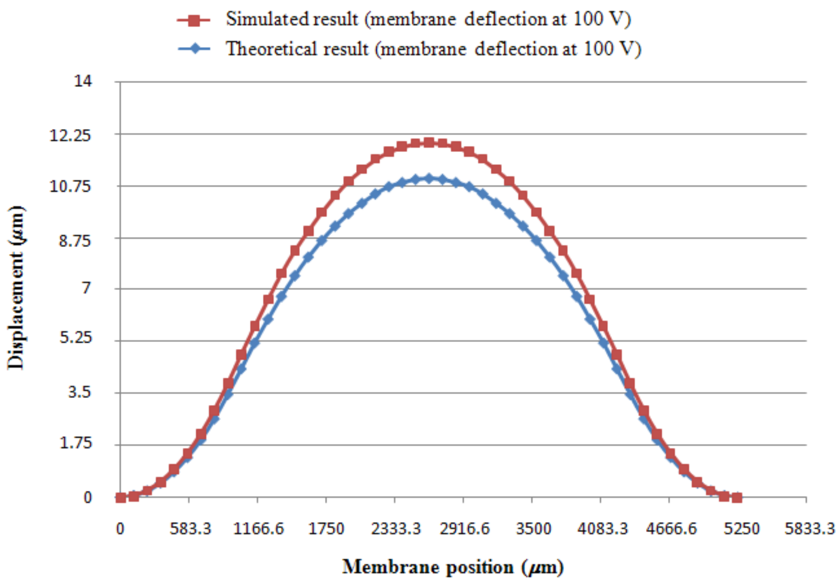

Fig. 15. Membrane deflection.

In FEM analysis the membrane deflection and frequencies relationship is shown by Fig. 16 at various applied voltages.

The flow rate for excitation frequencies at various applied voltages is shown by Fig. 17.

When the excitation frequency is increased, fluid flow rate also increases. The highest flow rate is achieved at applied 100 V.

In transient multifield analysis the fluid flow rate at applied 100 V with deflection of actuator 12.24 μm is shown by the Fig. 18.

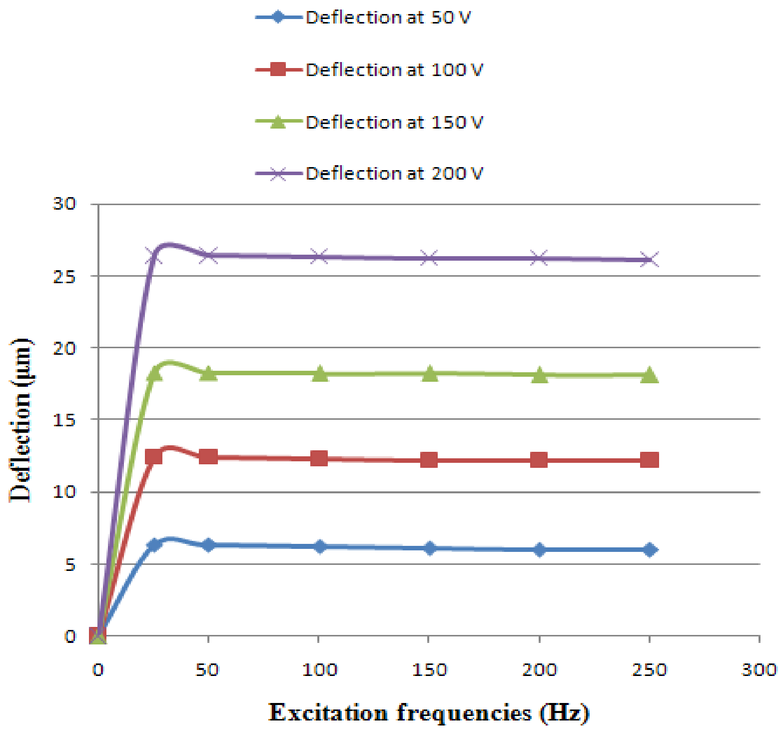

Fig. 16. Deflection of membrane at different applied voltages.

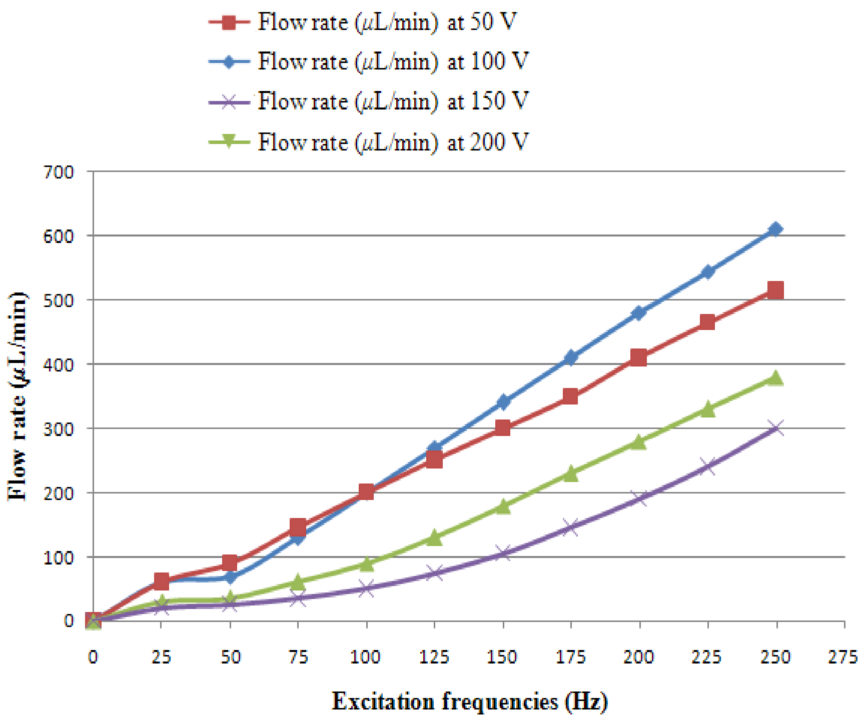

Fig. 17. Effect of frequencies on fluid flow at different applied voltages.

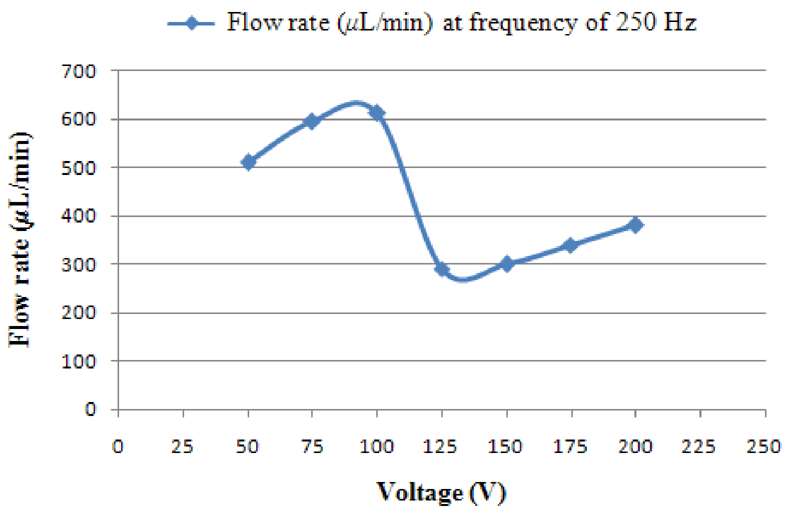

Fig. 18. Fluid flow rate at applied 100 V.

Fluid flow rate is effected by various factors like material properties, applied voltage, thickness of membrane and piezoelectric disk. The maximum flow rate of 612 μL/min is achieved through the 6×6 microneedle array at applied 100 V with membrane deflection of 12.24 μm.

6. Conclusions

In this study, fabrication of tapered tip hollow out-of-plane silicon microneedles is presented for TDD system. ICP technology is used to facilitate the fabrication of microneedles. Using ANSYS, structural and multiphysics analysis were performed to envisage the mechanical properties of microneedles and fluid flow rate through the microneedles. Numerical results show that the fabricated microneedles design is suitable for TDD. Microneedles can bear the bending and axial load during skin puncturing. Coupled multified analysis of piezoelectrically actuated device shows that piezoelectric-membrane assembly deflection increases with increase in excitation voltage but slowly decreases with increase in excitation frequency at the same voltage. Maximum fluid flow rate 612 μL/min is obtained at applied voltage of 100 V through 6×6 microneedle array with actuator deflection 12.24 μm. These fabricated microneedles can be integrated with our previously fabricated piezoelectric valveless micropump. The results of integrated microfluidic device will be shown in subsequent paper.

References

[1]. S. Henry, Microfabricated microneedles: a novel method to increase transdermal drug Delivery, *J. Pharm. Sci.*, 87, 1998, pp. 922– 925.

[2]. M. W. Ashraf, S. Tayyabal, N. Afzulpurkar, T. Lomas, A. Tuantranont, A. Nisar, and E. L. J. Bohez, Design, Analysis and Fabrication of MEMS-based Silicon Microneedles for Bio-Medical Applications, *ECTI-CON*, May 19- 21, 2010, Chiang Mai, Thailand.

[3]. P. K. Campbell, K. E. Jones, R. J. Huber, K. W. Horch and R. A. Normann, A silicon-based, three-dimensional neural interface: manufacturing processes for an intracortical electrode array, *IEEE Trans Biomed Eng.*, 38, 8, 1991, pp. 758-768.

[4]. C. S. Kolli and A. K. Banga, Characterization of Solid Maltose Microneedles and their Use for Transdermal Delivery, *Pharm. Res.*, 25, 2008, pp. 104-113.

[5]. T. Shibata, A. Nakanishi, T. Sakai, N. Kato, T. Kawashima, T. Mineta, and E. Makino, Fabrication and mechanical characterization of microneedle array for cell surgery, *in Proc. of the Actuators and Microsystems Conference*, pp. 719–722.

[6]. S. Khumpuang1, M. Horade, K. Fujioka, and S. Sugiyama, Geometrical StrEng., thening and tip-sharping of a microneedle array fabricated by X-ray lithography, *Microsist Technol.*, 13, pp. 209-214.

[7]. L. M. Yu, F. E. H. Tay, D. G. Guo, L. Xu, K. L. Yap, A microfabricated electrode with hollow microneedles for ECG measurements, *Sens Actuator A*, 151, 2009, pp. 17-22.

[8]. J. W. Lee, J. H. Park, M. R. Prausnitz, Dissolving microneedles for transdermal drug delivery, *Biomaterials*, 29, 2009, pp. 2113-2124.

[9]. P. Zhang, C. Dalton, and G. A. Jullien, Design and fabrication of MEMS-based microneedles arrays for medical applications, *Microsyst Technol*, 15, 2009, pp. 1073-1082.

[10]. Z. Ding, F. J. Verbaan, M. Bivas-Benita, L. Bungener, A. Huckriede, D. J. van den Berg, G. Kersten, J. A. Bouwstra, Microneedles arrays for the transcutaneous immunization of diphtheria and influenza in BALB/c mice, *J Control Release*, 136, 2009, pp. 71-78.

[11]. S. P. Davis, W. Martanto, M. G. Allen, and M. R. Prausnitz, Hollow metal microneedles for insulin delivery to diabetic rats, *IEEE Trans Biomed Eng.*, 52, 5, pp. 909–915.

[12]. J. Oh, H. Park, K. Doa, M. Han, D. Hyun, C. Kim, C. Kim, S. S. Lee, S. Hwang, S. Shin, C. Cho, Influence of the delivery systems using a microneedle array on the permeation of a hydrophilic molecule, calcein, Eur. *J. Pharm. Biopharm*, 69, 2009, pp. 1040-1045.

[13]. M. W. Ashraf, S. Tayyaba, N. Afzulpurkar, MEMS based Polymeric Drug Delivery System, in *Proc. of the 6th IEEE Conference on Automation Science and Engineering* (*CASE 2010)*, August 21- 24, 2010, Toronto, Canada.

[14]. R. Bhandari, S. Negi, L. Rieth, R. A. Norman, and F. Solzbacher, A Novel Mask-Less Method of Fabricating High Aspect Ratio Microneedles for Blood Sampling, in *Proc. of the IEEE, 2008 Electronic Components and Technology Conference*, pp. 1306-1309.

[15]. S. Rajaraman, and H. T. Henderson, A unique fabrication approach for microneedles using coherent porous silicon technology, *Sens. Actuator B*, 105, pp. 443-448.

[16]. F. Sammoura, J. Kang, Y. Heo, T. Jung and L. Lin, Polymeric microneedle fabrication using a microinjection molding technique, *Microsyst Techno*., 13, pp. 517-522.

[17]. J. Jiang, J. S. Moore, H. F. Edelhauser, and M. R. Prausnitz, Intrascleral Drug Delivery to the Eye Using Hollow Microneedles, *Pharm. Res.*, 26, pp. 395-403.

[18]. A. Nisar, N. Afzulpurkar, B. Mahaisavariya, A. Tuantranont, Multifield Analysis of a Piezoelectrically Actuated Valveless Micropump, *Sensors & Transducers*, Vol. 94, Issue 7, July 2008, pp. 176-195.

[19]. A. Nisar, N. Afzulpurkar, A. Tuantranont, B. Mahaisavariya, Three Dimensional Transient Multifield Analysis of a Piezoelectric Micropump for Drug Delivery System for Treatment of Hemodynamic Dysfunctions, *Cardiovasc Eng.*, 8, 2008, pp. 203–218.

[20]. W. S. Janna, Design of fluid thermal system: 2nd ed., *PWS Publications*, Boston, 1998.

[21]. P. Aggarwal and C. R. Johnston, Geomertrical effects in mechanical characterizing of microneedle for biomedical applications, *Sens Actuators B*, 102, 2004, pp. 226-234.

[22]. M. W. Ashraf, S. Tayyaba, A. Nisar, N. Afzulpurkar, and A. Tuantranont, Coupledfield Microfluidic Analysis of Integrated MEMS Based Device for Transdermal Drug, INMIC, in *Proc. of the 13th IEEE Multi-topic International Conference*, Islamabad, Pakistan, December 14-15, 2009.

[23]. N. Wilke, C. Hibert, J. O'Brien, and A. Morrissey, Silicon microneedle electrode array with temperature monitoring for electroporation, *Sensors and Actuators A*, 123–124, 2005, pp. 319–325.

[24]. X. Wang, X Chen, Z. Yu, and L. Wang, A novel fabrication approach for microneedles using silicon micromachining technology, in *Proc. of the 1st IEEE International Conference on Nano/Micro Engineered and Molecular Systems*, January 18 - 21, 2006, Zhuhai, China.

[25]. M. W. Ashraf, S. Tayyaba, N. Afzulpurkar, A. Nisar, A. Tuantranont, and E. L. J. Bohez, Coupled Multifield Analysis of *Piezoelectrically Actuated Microfluidic Device for Transdermal Drug Delivery Applications, in Proc. of the International Conference on Electrical Engineering (ICEE 2010)*, February 24 - 26, 2010, Penang, Malaysia.

[26]. M. W. Ashraf, S. Tayyaba, N. Afzulpurkar, A. K. Kasi, A. Nisar, and J. K. Kasi, MEMS based Biomedical Microfluidic Device, in *Proc. of the International Conference on Automation, Robotics and Control System*, July 12 – 14, 2010, Orlando, FL, USA.

Guide for Contributors

Aims and Scope

Sensors & Transducers Journal (ISSN 1726-5479) provides an advanced forum for the science and technology of physical, chemical sensors and biosensors. It publishes state-of-the-art reviews, regular research and application specific papers, short notes, letters to Editor and sensors related books reviews as well as academic, practical and commercial information of interest to its readership. Because it is an open access, peer review international journal, papers rapidly published in *Sensors & Transducers Journal* will receive a very high publicity. The journal is published monthly as twelve issues per annual by International Frequency Association (IFSA). In additional, some special sponsored and conference issues published annually. *Sensors & Transducers Journal* is indexed and abstracted very quickly by Chemical Abstracts, IndexCopernicus Journals Master List, Open J-Gate, Google Scholar, etc.

Topics Covered

Contributions are invited on all aspects of research, development and application of the science and technology of sensors, transducers and sensor instrumentations. Topics include, but are not restricted to:

- Physical, chemical and biosensors;
- Digital, frequency, period, duty-cycle, time interval, PWM, pulse number output sensors and transducers;
- Theory, principles, effects, design, standardization and modeling;
- Smart sensors and systems;
- Sensor instrumentation;
- Virtual instruments;
- Sensors interfaces, buses and networks;
- Signal processing;
- Frequency (period, duty-cycle)-to-digital converters, ADC;
- Technologies and materials;
- Nanosensors;
- Microsystems;
- Applications.

Submission of papers

Articles should be written in English. Authors are invited to submit by e-mail editor@sensorsportal.com 8-14 pages article (including abstract, illustrations (color or grayscale), photos and references) in both: MS Word (doc) and Acrobat (pdf) formats. Detailed preparation instructions, paper example and template of manuscript are available from the journal's webpage: http://www.sensorsportal.com/HTML/DIGEST/Submition.htm Authors must follow the instructions strictly when submitting their manuscripts.

Advertising Information

Advertising orders and enquires may be sent to sales@sensorsportal.com Please download also our media kit: http://www.sensorsportal.com/DOWNLOADS/Media_Kit_2009.pdf